Journal of Solid State Chemistry **156,** 1–9 (2001)
doi:10.1006/jssc.2000.8917, available online at http://www.idealibrary.com on IDEAL®

Subcell Structure and Two Different Superstructures of the Rare Earth Metal Silicide Carbides $Y_3Si_2C_2$, $Pr_3Si_2C_2$, $Tb_3Si_2C_2$, and $Dy_3Si_2C_2$

Wolfgang Jeitschko, Martin H. Gerdes, Anne M. Witte, and Ute Ch. Rodewald

Anorganisch-Chemisches Institut, Universität Münster, Wilhelm-Klemm-Strasse 8, D-48149 Münster, Germany

Received March 20, 2000; in revised form July 25, 2000; accepted August 9, 2000; published online January 3, 2001

The title compounds crystallize with a very pronounced subcell structure that has been determined from single-crystal X-ray diffractometer data of all four compounds. Only subcell (and no superstructure) reflections have been observed for $Pr_3Si_2C_2$: space group *Cmmm*, $a = 396.7(1)$ pm, $b = 1645.2(3)$ pm, $c = 439.9(1)$ pm, $R = 0.019$ for 309 structure factors and 20 variable parameters. In this subcell structure there are C_2 pairs with split atomic positions. This structure may be considered the thermodynamically stable form of these compounds at high temperatures. Two different superstructures with doubled *a* or *c* axes, respectively, of the subcell have been observed, where the C_2 pairs have different orientations. In the structure of $Tb_3Si_2C_2$ the *a* axis of the subcell is doubled. The resulting superstructure in the standard setting has the space group *Pbcm*: $a = 423.6(1)$ pm, $b = 770.7(1)$ pm, $c = 1570.2(3)$ pm, $R = 0.031$ for 1437 structure factors and 22 variable parameters. $Dy_3Si_2C_2$ has the same superstructure: $a = 420.3(1)$ pm, $b = 767.5(1)$ pm, $c = 1561.1(3)$ pm, $R = 0.045$, 801 *F* values, 22 variables. In the structure of $Y_3Si_2C_2$ the *c* axis of the subcell is doubled, resulting in a body- centered space group with the standard setting *Imma*: $a = 842.6(2)$ pm, $b = 1563.4(2)$ pm, $c = 384.6(1)$ pm, $R = 0.035$, 681 *F* values, 15 variables. In all of these structures the rare earth atoms form two-dimensionally infinite sheets of edge-sharing octahedra that contain the C_2 pairs. In between these sheets there are zig-zag chains of silicon atoms with Si–Si distances varying between 246.2(3) and 253.6(3) pm, somewhat longer than the two-electron bonds of 235 pm in elemental silicon, suggesting a bond order of 0.5 for the Si–Si bonds. The C–C distances in the C_2 pairs vary between 127(1) and 131(1) pm, corresponding to a bond order of approximately 2.5. Hence, using oxidation numbers, the compounds may to a first approximation be represented by the formula $(R^{+3})_3(Si^{-3})_2(C_2)^{-3}$. A more detailed analysis of the interatomic distances shows that the shortest *R–R* distances are comparable with the *R–R* distances in the structures of the rare earth elements, thus indicating some *R–R* bonding. Therefore, the oxidation numbers of the rare earth atoms are slightly lower than + 3, in agreement with the metallic conductivity of these compounds. As a consequence, considering the relatively short Si–Si bonds, the absolute value of the oxidation number of the silicon atoms may be lower than 3, resulting in a Si–Si bond order somewhat higher than 0.5. © 2001 Academic Press

INTRODUCTION

We have recently reported on the electrical and magnetic properties of a new series of rare earth silicide carbides $R_3Si_2C_2$ (R = Y, La–Nd, Sm, Gd–Tm). These 12 compounds show metallic conductivity and their magnetic ordering temperatures are all lower than 60 K. They were found to crystallize with at least two slightly different structures with a common subcell. The lattice constants for this orthorhombic subcell have already been published (1). In the present paper we report the structure of the subcell and two different superstructures. Only the subcell (and no long-range order corresponding to a superstructure) was found for $Pr_3Si_2C_2$; one superstructure was observed for $Y_3Si_2C_2$ and another one for $Tb_3Si_2C_2$ and $Dy_3Si_2C_2$. The superstructures differ essentially only in the orientation of the C_2 dumbbells. A brief account of the structure of $Tb_3Si_2C_2$ has been presented at a conference (2). The compounds are stable on air. For the sample preparation the reader is referred to the earlier publication (1).

LATTICE CONSTANTS

Single crystals of the four compounds $R_3Si_2C_2$ (R = Y, Pr, Tb, Dy) were selected from the polycrystalline samples on the basis of Laue diffraction patterns. They were mounted on a four-circle diffractometer. The crystal of $Tb_3Si_2C_2$ was investigated first, and the search routine of the diffractometer resulted in the correct orthorhombic cell dimensions of the superstructure: $a = 423.1(1)$ pm, $b = 771.4(1)$ pm, $c = 1570.4(4)$ pm. Analogous cell dimensions were found for $Dy_3Si_2C_2$: $a = 420.7(1)$ pm, $b = 767.5(2)$ pm, $c = 1559.7(5)$ pm. For $Y_3Si_2C_2$ the single-crystal diffractometer data resulted in a body-centered orthorhombic cell: $a = 842.2(2)$ pm, $b = 1563.7(3)$ pm, $c = 384.7(1)$ pm.

The structure determinations of these three compounds showed that they crystallize with a very pronounced common orthorhombic subcell. For the crystal of the praseodymium compound only subcell reflections were observed,

0022-4596/01 $35.00

despite time-consuming attempts to search for various superstructures. The lattice constants for this subcell of $Pr_3Si_2C_2$, found with the data from the four-circle diffractometer, are as follows: $a = 396.63(2)$ pm, $b = 1645.1(1)$ pm, $c = 440.34(3)$ pm.

The Guinier powder patterns of these compounds are dominated by the subcell reflections, while the strongest superstructure reflections are barely visible. In Table 1 we list the lattice constants as obtained from the Guinier data, after doubling the appropriate cell dimensions, as found from the single-crystal investigations. It can be seen that the agreement between the lattice constants listed above and the lattice constants of Table 1 is very good in all cases.

STRUCTURE DETERMINATIONS

Intensity data were recorded on an Enraf-Nonius CAD4 four-circle diffractometer with graphite-monochromated Mo$K\alpha$ radiation at room temperature using a scintillation counter with pulse height discrimination and $\theta/2\theta$ scans with background counts at both ends of each scan. Empirical absorption corrections were made on the basis of psi scan data. Further details of the data collections are summarized in Table 1.

The structures were determined with the program packages SDP (3), SHELXS-86 (4), and SHELXL-93 (5). The final full-matrix least-squares refinements were all done with the SHELX-97 package (6) with atomic scattering factors as provided by that program. The weighting schemes accounted for the counting statistics and a parameter correcting for isotropic secondary extinction was optimized during the least-squares refinements. The results are summarized in Tables 1–3.

The structure of $Tb_3Si_2C_2$ was determined first. The space group *Pbcm* suggested by the computer software was confirmed during the final least-squares refinements. The positions of the terbium atoms were obtained from a Patterson synthesis and the light atoms were located from difference Fourier analyses. The structure refinements with the least-squares programs resulted in some difficulties for the Tb2 position, especially in refinements with anisotropic displacement parameters. The most satisfactory refinement was obtained by splitting this position into a Tb2a and a Tb2b position and refining it with constrained isotropic displacement parameters. The refinement of the occupancy parameters showed that 90.2(1)% of the scattering power originated from the Tb2a position and only 9.8(1)% from the Tb2b position.

TABLE 1
Crystal Data and Results of the Structure Refinements for the Subcells and the Superstructures of the Silicide Carbides $R_3Si_2C_2$ (R = Y, Pr, Tb, and Dy)

Empirical formula	$Pr_3Si_2C_2$	$Tb_3Si_2C_2$		$Dy_3Si_2C_2$		$Y_3Si_2C_2$	
Formula mass	502.9	557.0		567.7		346.9	
Calculated density (g cm^{-3})	5.82	7.22		7.49		4.55	
Crystal size (μm^3)	$44 \times 66 \times 100$	$20 \times 30 \times 90$		$40 \times 66 \times 66$		$88 \times 44 \times 22$	
2θ range up to (°)	65	90		70		80	
Max/min transmission	1.51	1.29		1.29		1.97	
	Subcell	Subcell	Superstructure	Subcell	Superstructure	Subcell	Superstructure
Space group	*Cmmm*	*Cmmm*	*Pbcm*	*Cmmm*	*Pbcm*	*Cmmm*	*Imma*
a (pm)	396.7(1)	385.4(1)	423.6(1)	383.8(1)	420.3(1)	384.6(1)	842.6(1)
b (pm)	1645.2(3)	1570.2(2)	770.7(1)	1561.1(3)	767.5(1)	1563.4(2)	1563.4(2)
c (pm)	439.9(1)	423.6(1)	1570.2(3)	420.3(1)	1561.1(3)	421.3(1)	384.6(1)
V (nm)^3	0.28710	0.25634	0.51262	0.25181	0.50358	0.25332	0.50664
Formula units/cell	2	2	4	2	4	2	4
Range in *hkl*	$\pm5, \pm24, 6$	$\pm7, 31, \pm8$	$\pm8, \pm15, 31$	$\pm6, 0–25, \pm6$	$\pm6, \pm12, -25/13$	$\pm6, -27/4, \pm7$	$\pm15, -27/4, \pm6$
Total no. of reflections	1125	2111	7906	1132	4217	1864	3539
Independent reflections	324	643	2167	351	1132	484	843
Reflections with $I_o > 2\sigma(I_o)$	309	598	1437	341	801	421	681
$R_{int}(F^2)$	0.048	0.038	0.056	0.086	0.099	0.034	0.047
Variables	20	20	22	20	22	20	15
$R(F > 2\sigma)^a$	0.019	0.017	0.031	0.027	0.045	0.043	0.035
R_w(all F^2)^a	0.057	0.057	0.107	0.071	0.132	0.100	0.102
Highest resid. peaks (e/Å^3)	2.4; 1.4	6.4; 2.4	12.2; 5.9	4.0; 3.8	7.3; 6.6	8.9; 4.3	3.2; 2.7
Superstr. refl. with $I_o > 2\sigma(I_o)$	—	—	839	—	463	—	260
Corresponding $R(F)^a$	—	—	0.050	—	0.086	—	0.059

$^a R(F)$ is defined as $R(F) = \sum||F_o| - |F_c||/\sum F_o$; R_w is defined as $R_w = \{\sum[w(F_o^2 - F_c^2)^2]/\sum[w(F_o^2)^2]\}^{1/2}$.

TABLE 2
Atomic Parameters for the Subcell Structure of the Silicide Carbides $R_3Si_2C_2$ (R = Y, Pr, Tb, and Dy)[a]

	$Pr_3Si_2C_2$	$Tb_3Si_2C_2$	$Dy_3Si_2C_2$	$Y_3Si_2C_2$
*R*1				
x	0	0	0	0
y	0.34523(2)	0.34531(1)	0.34515(3)	0.34536(3)
z	1/2	1/2	1/2	1/2
U_{11}	28(2)	55(1)	28(2)	59(1)
U_{22}	52(2)	45(1)	26(2)	52(1)
U_{33}	73(2)	60(1)	26(2)	59(1)
U_{eq}	51(2)	53(1)	27(2)	57(1)
*R*2				
x	0	0	0	0
y	0	0	0	0
z	0.0504(1)	0.0510(1)	0.0499(2)	0.0241(4)
U_{11}	36(3)	112(1)	52(3)	720(8)
U_{22}	71(3)	57(1)	40(3)	46(2)
U_{33}	88(6)	99(2)	41(8)	100(4)
U_{eq}	65(2)	90(1)	44(3)	289(3)
Si				
x	0	0	0	0
y	0.2028(1)	0.1997(1)	0.1994(2)	0.1990(1)
z	0	0	0	0
U_{11}	29(7)	57(4)	28(10)	80(4)
U_{22}	84(7)	62(4)	54(11)	65(4)
U_{33}	81(7)	66(4)	26(10)	62(4)
U_{eq}	64(3)	62(2)	36(5)	69(2)
C				
x	0.397(2)	0.394(2)	0.394(4)	0.381(2)
y	0	0	0	0
z	0.384(2)	0.382(2)	0.379(4)	0.391(2)
U_{11}	38(30)	141(22)	64(43)	212(27)
U_{22}	99(31)	57(18)	3(38)	70(20)
U_{33}	106(32)	146(25)	97(57)	158(25)
U_{13}	13(31)	− 27(20)	19(50)	− 44(25)
U_{eq}	81(14)	115(9)	55(22)	147(13)

[a] The *R*1 and Si atoms occupy the Wyckoff positions 4*j* and 4*i*, respectively, of the space group *Cmmm* (No. 65). The *R*2 and C atoms are at the split positions 4*k* and 8*o* with occupancies of one half. Only the displacement parameters U_{ij} (pm^2) that are different from zero are listed. They are defined by $\exp(-2\pi^2[h^2(a^*)^2U_{11} + \cdots + 2klb^*c^*U_{23}])$.

At this point we still assumed that the whole series of the rare earth silicide carbides $R_3Si_2C_2$ crystallizes with isotypic crystal structures. We therefore investigated crystals of the presumably isotypic other compounds, hoping that the difficulties found with the Tb2 position would not arise in crystals with other rare earth elements. For the dysprosium compound we indeed found a similar unit cell and the least-squares refinement for $Dy_3Si_2C_2$ resulted in atomic positions corresponding to those of $Tb_3Si_2C_2$. However, again the rare earth atoms (*R*) of the Wyckoff position 4*d* had to be refined as split positions. But, in contrast to the positions of the *R*1, Si, and C atoms, which exactly correspond to each other in the two compounds $Tb_3Si_2C_2$ and $Dy_3Si_2C_2$, the *R*2 positions, especially the *R*2b positions of the two compounds, differ somewhat. These Tb2b and Dy2b positions may be ascribed to domains of one or the other superstructure, which is discussed further below. The occupancy parameters of these positions amount to only about 10%, and the superstructures differ essentially only in the positions of the *R*2 atoms and in the orientation of the C_2 pairs. However, the split positions for the carbon atoms are not observed in the difference Fourier syntheses, because of the weak scattering power of the carbon atoms.

The highest peaks in the final difference Fourier syntheses of the two compounds (12.2 e/Å^3 and 7.3 e/Å^3 for $Tb_3Si_2C_2$ and $Dy_3Si_2C_2$, respectively) are both in the vicinity of the Tb2a (50 pm), Tb2b (53 pm), Dy2a (72 pm), and Dy2b (50 pm) positions. These distances are similar to the distances between the split positions of 34.9(2) pm for Tb2a–Tb2b and 45.5(5) pm for Dy2a–Dy2b. Hence, the highest peaks of the difference Fourier analyses can again be ascribed to the presence of domains of another superstructure. It may also be, that in some parts of the investigated crystals the superstructure is not fully developed.

The structure determination of $Y_3Si_2C_2$ resulted in a different superstructure with a large body-centered orthorhombic cell of the space group *Imma*, again with a split position for one of the yttrium atoms with occupancies of 91.8(3) and 8.2(3)% for Y2a and Y2b, respectively. The

TABLE 3
Atomic Parameters for the Superstructures of the Silicide Carbides $Tb_3Si_2C_2$, $Dy_3Si_2C_2$, and $Y_3Si_2C_2$[a]

Atom	Occupancy	Site	*x*	*y*	*z*	*U*
$Tb_3Si_2C_2$ (space group *Pbcm*, No. 57)						
Tb1	1	8*e*	0.50080(2)	0.37499(3)	0.09531(1)	48.0(2)
Tb2a	0.902(1)	4*d*	0.05318(5)	0.12488(3)	1/4	67.0(3)
Tb2b	0.098	4*d*	0.9834(5)	0.1009(3)	1/4	67.0
Si	1	8*e*	0.0034(2)	0.1253(2)	0.05024(6)	57(1)
C1	1	4*d*	0.6193(11)	0.3213(6)	1/4	102(6)
C2	1	4*d*	0.3816(11)	0.4291(6)	1/4	94(6)
$Dy_3Si_2C_2$ (space group *Pbcm*, No. 57)						
Dy1	1	8*e*	0.50072(6)	0.37510(14)	0.09517(2)	12(1)
Dy2a	0.891(1)	4*d*	0.0492(1)	0.1249(1)	1/4	23(1)
Dy2b	0.109	4*d*	0.9415(11)	0.1184(8)	1/4	23
Si	1	8*e*	0.0017(4)	0.1251(9)	0.0504(1)	24(3)
C1	1	4*d*	0.618(3)	0.325(1)	1/4	73(17)
C2	1	4*d*	0.383(3)	0.428(1)	1/4	70(17)
$Y_3Si_2C_2$ (space group *Imma*, No. 74)						
Y1	1	8*g*	1/4	0.59534(3)	1/4	50(1)
Y2a	0.918(3)	4*e*	0	1/4	0.1936(3)	98(2)
Y2b	0.082	8*i*	0.0413(10)	1/4	0.2585(17)	98
Si	1	8*h*	0	0.0510(1)	0.2437(3)	60(2)
C	1	8*i*	0.1953(7)	1/4	0.6300(14)	130(9)

[a] The Tb2, Dy2, and Y2 positions were refined with split occupancy. No standard deviations are listed for dependent parameters. All atomic positions were refined with isotropic displacement parameters *U* (pm^2).

corresponding Y2a–Y2b distance is again quite short: 42.8(8) pm. Because of the different symmetry, there is also an (impossibly) short Y2b–Y2b distance of 70(2) pm. Again, the Y2b positions can be ascribed to domains of another superstructure or to disorder. In contrast to the structure refinements of $Tb_3Si_2C_2$ and $Dy_3Si_2C_2$, the final difference Fourier syntheses of $Y_3Si_2C_2$ showed no high residual electron density and the highest peak of 3.2 e/Å^3 is not in the vicinity of an yttrium atom.

The structures of the isotypic compounds $Tb_3Si_2C_2$ and $Dy_3Si_2C_2$ on the one hand, and that of $Y_3Si_2C_2$ on the other, are very similar, and they have a common subcell that was recognized during the structure refinements. For $Pr_3Si_2C_2$ only this subcell was found. The corresponding atomic parameters are listed in Table 2 together with the parameters of the subcells of the other three structure refinements. These subcell refinements were all carried out with anisotropic displacement parameters, in contrast to the last refinement cycles of the superstructures where isotropic displacement parameters were used (Table 3). This may explain the fact that the highest peaks in the difference Fourier syntheses of $Tb_3Si_2C_2$ and $Dy_3Si_2C_2$ (Table 1) are greater for the refinements of the superstructures than those for the refinements of the subcells. The interatomic distances listed in Table 4 are those of the final refinements of the subcell for $Pr_3Si_2C_2$ and of the superstructures for the other three compounds. The interatomic distances to and from the *R*2b sites (ascribed to domains with differing orientations of the C_2 pairs) are not listed. In assessing the quality of the structure refinements of the superstructures the residuals obtained for the whole structure are poor indicators, because these residuals are dominated by the agreement of the strong subcell reflections. For that reason we have also calculated (8) separate conventional residuals (on *F* values) for the superstructure reflections. They are listed in the last line of Table 1. As can be seen, despite the poor counting statistics of these weak reflections, they are all smaller than 9%, thus indicating that the superstructures are correct.

DISCUSSION

The series of rare earth silicide carbides $R_3Si_2C_2$ are represented in Fig. 1 through the cell volumes of their orthorhombic subcells. The positional parameters of the subcells of the four refined structures are practically the same (Table 2). Our single-crystal investigations revealed two different superstructures. One where the *a* axis of the subcell is doubled. This superstructure was found for $Tb_3Si_2C_2$ and $Dy_3Si_2C_2$. The other superstucture was found for $Y_3Si_2C_2$. In this structure the *c* axis of the subcell is doubled. We could not detect any superstructure reflections for the crystal of $Pr_3Si_2C_2$. However, we assume at least short-range order for this compound corresponding to one or the other superstructure. In this context it is

TABLE 4
Interatomic Distances in the Structures of $R_3Si_2C_2$ (R = Pr, Tb, Dy, Y)[a]

	$Pr_3Si_2C_2$			$Tb_3Si_2C_2$	$Dy_3Si_2C_2$		$Y_3Si_2C_2$	
Pr1:	4/2C	262.9	*R*1:	1C1	251.5	249.7	Y1: 2C	250.4
	4Si	306.5		1C2	251.6	250.0	2Si	291.9
	2Si	321.4		1Si	293.8	292.3	2Si	295.1
	2Pr1	370.9		1Si	294.0	292.7	2Si	311.1
	4/2Pr2	378.5		1Si	295.6	293.3	2Y1	354.8
	2Pr1	396.7		1Si	296.4	293.8	2Y2a	363.2
	4/2Pr2	403.5		1Si	310.8	309.3	2Y1	384.6
	2Pr1	439.9		1Si	312.3	309.8	2Y2a	385.5
Pr2:	(1Pr2	44.4)		1*R*1	355.9	353.6	2Y1	421.3
	(2C	215.2)		1*R*1	356.0	353.8	Y2a: 2C	235.1
	2C	247.5		1*R*2a	363.0	361.9	2C	272.1
	2C	280.7		1*R*2a	363.5	362.4	2C	285.3
	2C	294.4		2*R*1	385.4	383.8	2Si	311.7
	(2C	306.2)		1*R*2a	388.5	385.3	4Y1	363.2
	(2C	332.8)		1*R*2a	388.8	385.5	2Y2a	384.6
	2Si	334.4		2*R*1	423.6	420.3	4Y1	385.5
	(2C	345.2)	*R*2a:	1C2	238.1	236.4	2Y2a	423.5
	4Pr1	378.5		1C1	238.1	237.3	Si: 1Si	246.2
	1Pr2	395.5		1C1	272.0	269.4	1Si	253.6
	2/2Pr2	396.7		1C2	272.6	271.8	2Y1	291.9
	2/2Pr2	399.2		1C2	283.0	282.3	2Y1	295.1
	4Pr1	403.5		1C1	283.6	284.2	2Y1	311.1
	2/2Pr2	439.9		2Si	314.4	312.2	1Y2a	311.7
Si:	2Si	251.9		2*R*1	363.0	361.9	C: 1C	130.5
	4Pr1	306.5		2*R*1	363.5	362.4	1Y2a	235.1
	2Pr1	321.4		2*R*2a	388.0	386.0	2Y1	250.4
	2/2Pr2	334.4		2*R*1	388.5	385.3	1Y2a	272.1
C:	(1C	81.9)		2*R*1	388.8	385.5	1Y2a	285.3
	(1C	102.2)		2*R*2a	423.6	420.3		
	1C	131.0	Si:	1Si	248.7	248.1		
	(1Pr2	215.2)		1Si	249.4	248.4		
	1Pr2	247.5		1*R*1	293.8	292.3		
	2Pr1	262.9		1*R*1	294.0	292.7		
	1Pr2	280.7		1*R*1	295.6	293.3		
	1Pr2	294.4		1*R*1	296.4	293.8		
	(1Pr2	306.2)		1*R*1	310.8	309.3		
	(1Pr2	332.8)		1*R*1	312.3	309.8		
	(1Pr2	345.2)		1*R*2a	314.4	312.2		
			C1:	1C2	130.5	126.6		
				1*R*2a	238.1	237.3		
				2*R*1	251.5	249.7		
				1*R*2a	272.0	269.4		
				1*R*2a	283.6	284.2		
			C2:	1C1	130.5	126.6		
				1*R*2a	238.1	236.4		
				2*R*1	251.6	250.0		
				1*R*2a	272.6	271.8		
				1*R*2a	283.0	282.3		

[a] These distances were calculated using the lattice constants of Table 1 obtained from the powder data. For the three compounds $Tb_3Si_2C_2$, $Dy_3Si_2C_2$, and $Y_3Si_2C_2$ only distances in the major domain are listed. Hence the distances to and from the *R*2b positions, which are ascribed to twin domains with occupancies of only 9.8(1)% (Tb2b), 10.9(1)% (Dy2b), and 8.2(3)% (Y2b), are not listed. All distances shorter than 480 pm (*R*–*R*), 360 pm (*R*–Si, *R*–C, Si–Si, Si–C), and 300 pm (C–C) are listed. Standard deviations are equal or smaller than 0.3 pm for the heavy atoms in $Pr_3Si_2C_2$, $Tb_3Si_2C_2$, and $Y_3Si_2C_2$ and less than 1.1 pm for $Dy_3Si_2C_2$. Interatomic distances for carbon atoms have standard deviations all smaller than 2.0 pm. Interatomic distances of $Pr_3Si_2C_2$ listed in parentheses are between sites with partial occupancy and do not occur in the ordered structures.

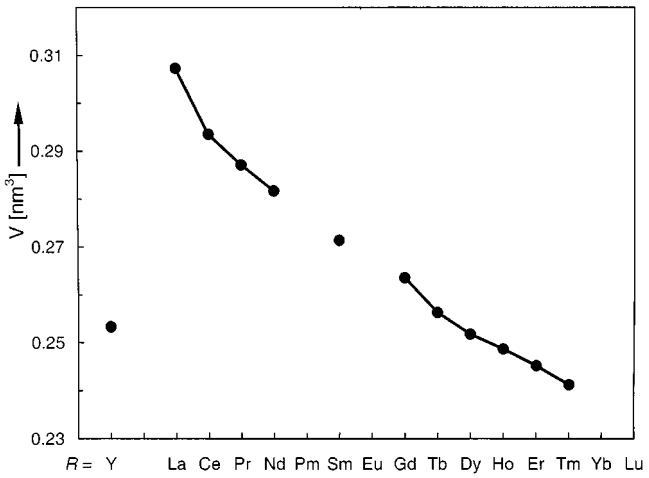

FIG. 1. Cell volumes of the subcells of the carbides $R_3Si_2C_2$.

worthwhile to remember the Scherrer formula for the determination of the particle size from line broadening (9–11). In using this formula one can estimate that superstructure reflections are detectable only if the domains of the ordered superstructure exceed 3000 pm in diameter.

In Fig. 2 we compare the atomic positions of the subcell (as determined for $Pr_3Si_2C_2$) and the two superstructures. It can be seen that the two superstructures as determined for $Tb_3Si_2C_2$ and $Y_3Si_2C_2$ differ essentially only in the orientation of the C_2 pairs. The positions of the neighboring *R*2 atoms are somewhat affected by the orientation of the C_2 pairs, while the positions of the *R*1 and the silicon atoms are essentially the same in the subcell as well as in the two superstructures. In the structure of the subcell (shown for $Pr_3Si_2C_2$) both orientations of the C_2 pairs were found superimposed with occupancies of one half, and the *R*2 atoms had to be refined with split positions.

The structure of the subcell is most likely the thermodynamically stable modification for all of these rare earth silicide carbides at high temperature with dynamic disorder for the orientation of the C_2 dumbbells, as this is known for the high-temperature modifications of CaC_2 and KCN (12). At lower temperatures the thermal motion of the C_2 dumbbells is frozen in, resulting in the superstructures. Corresponding superstructure reflections can only be observed if the domain sizes are large enough, as already mentioned above. These domains have to be considered as antiphase domains, since those parts of the structures containing the

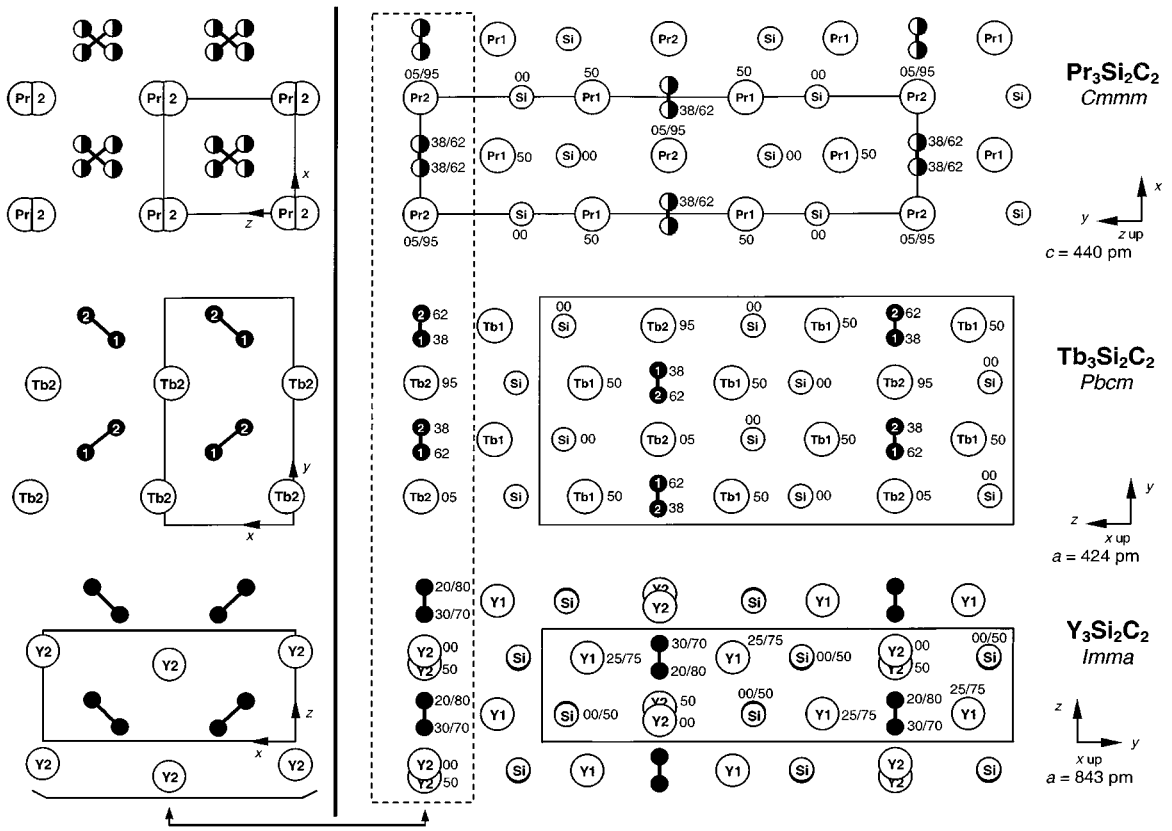

FIG. 2. Crystal structures of the rare earth silicide carbides $Pr_3Si_2C_2$, $Tb_3Si_2C_2$, and $Y_3Si_2C_2$. For $Pr_3Si_2C_2$ (top) only the subcell with disordered half-occupied carbon positions was observed. In the other two structures the C_2 pairs are ordered leading to doubling of differing translation periods. The main differences in the structures occur for the atoms that are enclosed with dashed lines. These are shown on the left-hand side in a different projection.

*R*1 and the Si atoms have the same orientation in the subcell and in all domains of the superstructures. The transformations from the (high-temperature) subcell structures to the superstructures are *klassengleich*; i.e., the subcell and the superstructures all belong to the same crystal class *mmm*. The superstructures arise through the loss of translational symmetry. In contrast, twin domains would be expected, if the phase transitions from the high-temperature disordered structures to the low-temperature ordered structures were associated with a loss of rotational symmetry (13).

The cell volume per formula unit of $Y_3Si_2C_2$ (0.12666 nm^3) is in between those of the two isotypic compounds $Tb_3Si_2C_2$ (0.12815 nm^3) and $Dy_3Si_2C_2$ (0.12589 nm^3). Therefore, the size of the rare earth atoms is not the only factor determining which kind of superstructure is adopted. Actually, it is possible to envision more complicated patterns for the orientation of the C_2 pairs and therefore the two different superstructures found by us may not be the only ones. Other superstructures could possibly occur for some of the other compounds of the series $R_3Si_2C_2$, which we have not investigated by single-crystal diffractometry. As already mentioned above, it is difficult to distinguish the superstructures from powder patterns. The intensities of the strongest superstructure reflections—as calculated with the positional parameters of the refined structures (14)—amount to only 2% of the intensities of the strongest subcell reflections.

In principle, the crystal structures of the rare earth silicide carbides $R_3Si_2C_2$ are rather simple (Fig. 3). The C_2 pairs are octahedrally coordinated by rare earth atoms. These R_6C_2 octahedra share four of their *R* atoms with four neighboring octahedra, thus forming two-dimensionally infinite sheets with the composition R_3C_2. In Fig. 4 these sheets of edge-sharing R_6 octahedra are shown in views along directions perpendicular to the sheets. In between these sheets—in the grooves of the edge-sharing R_6 octahedra—there are zig-zag chains of silicon atoms. There are no Si–C bonds in the structures of the rare earth silicide carbides $R_3Si_2C_2$, in contrast to the structure of the corresponding uranium compound $U_3Si_2C_2$, where the silicon atoms form SiC units, which are coordinated only by (nine) uranium atoms (16).

The near-neighbor environments of the two different superstructures of $Tb_3Si_2C_2$ and $Y_3Si_2C_2$ are practically the same (Fig. 5) even though the site symmetries of all atoms are higher in the yttrium compound than in the terbium compound. The two different kinds of rare earth atoms of both structures have large coordination numbers. The *R*1 atoms have close contacts to 2 carbon and 6 silicon atoms, and the *R*2 atoms have 6 carbon and 2 silicon neighbors. In addition, the *R*1 and *R*2 atoms have 10 and 12 *R* atoms, respectively, in their coordination shells. The *R*–*R* distances range from 355.9(1) to 423.6(1) pm for $Tb_3Si_2C_2$, from 353.6(1) to 420.3(1) pm for $Dy_3Si_2C_2$, and from 354.8(1) to 423.5(1) pm for $Y_3Si_2C_2$. At least the shorter ones of these *R*–*R* interactions must be ascribed some (weakly) bonding character, since they are shorter than the average interatomic distances in the structures of the elements: $2r$(Tb) = 356.6 pm, $2r$(Dy) = 354.8 pm, $2r$(Y) = 360.2 pm, as calculated by us from the lattice constants of the rare earth elements compiled by Donohue (17). Such a comparison might not be appropriate if the anionic part (the silicon and carbon atoms) of the compounds $R_3Si_2C_2$ had higher electronegativity. For instance, in a rare earth oxide the *R*–*R* distances should be compared with the ionic radii of the *R* elements. These are much smaller than the metallic radii. However, in the compounds $R_3Si_2C_2$ the valence electrons of the rare earth elements forming the bonds to the silicon and carbon atoms have more covalent character and a comparison of the *R*–*R* distances with the metallic radii of the rare elements is instructive.

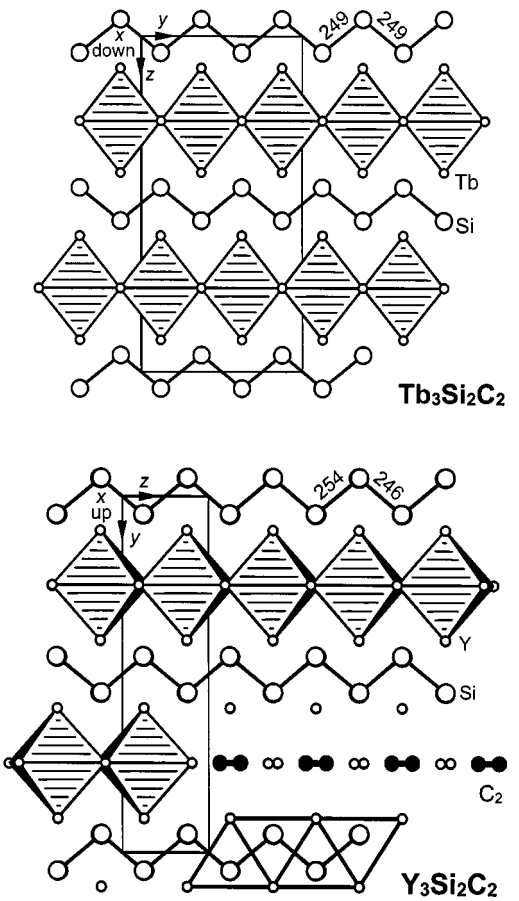

FIG. 3. The crystal structures of $Tb_3Si_2C_2$ and $Y_3Si_2C_2$ emphasizing the silicon chains and the octahedra of rare earth atoms surrounding the C_2 pairs. In the structure of $Y_3Si_2C_2$ the translation period *a* (along the viewing direction) is twice as large as in the structure of $Tb_3Si_2C_2$. The trigonal prisms of yttrium atoms around the silicon atoms are outlined at the bottom of the figure. The program DIAMOND (15) was used for drawing this figure.

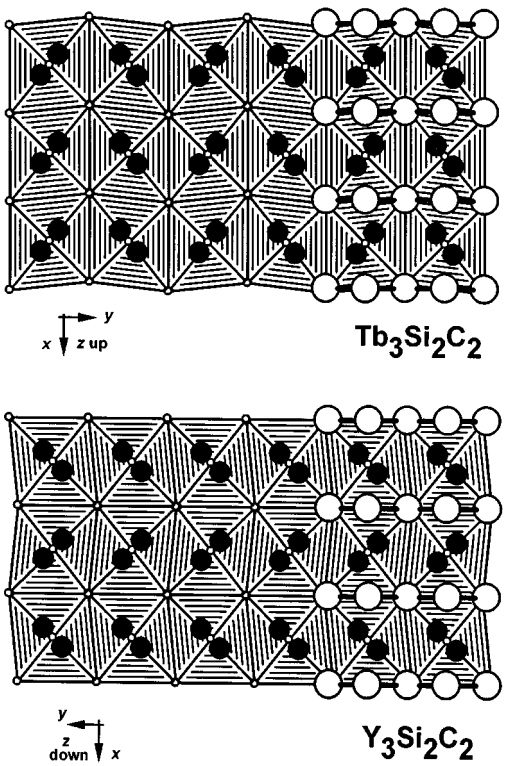

FIG. 4. Cutouts from the two-dimensionally infinite sheets of edge-sharing R_6 octahedra containing the C_2 pairs. In the superstructures of $Tb_3Si_2C_2$ and $Y_3Si_2C_2$ these C_2 dumbbells have differing orientations. On the right-hand sides of the drawings the zig-zag chains of silicon atoms in front of the sheets of R_6 octahedra are shown.

The silicon atoms are located in trigonal prisms formed by rare earth atoms. The three rectangular faces of these prisms are capped by two silicon and one rare earth atom. Hence, the silicon atoms have the coordination number 9. We discuss the Si–Si bonding below.

The carbon atoms are coordinated by five rare earth atoms and one carbon atom. Together these six neighbors of a carbon atom form a very distorted octahedron. However, a better way of looking at the carbon atoms is to consider them as C_2 pairs that are located in rare earth octahedra. The C–C distances in the four refined structures are practically the same with 131(2), 130.5(6), 127(1), and 130(1) pm for the Pr, Tb, Dy, and Y compounds, respectively. These may be compared with the triple-bond distance of 120 pm in acetylene and the double-bond distance of 134 pm in ethylene. Thus, we can estimate the oxidation number (formal charges, where the bonding electrons are *counted* at the atoms with the higher electronegativity, irregardless of their more or less covalently bonding character) of the C_2 pairs in the compounds $R_3Si_2C_2$ to be in between those of the C_2 pairs in acetylene (-2) and ethylene (-4). In aiming for integer numbers (not a requirement for the band structure of a solid) we assign the oxidation number -3 to the C_2 pairs in the compound $R_3Si_2C_2$.

The silicon atoms in these compounds form zig-zag chains. The seven different Si–Si bond distances, determined in the four structure refinements, range in between 246.2(3) and 253.6(3) pm. Both of these extreme values were found for the yttrium compound. In contrast, in $Tb_3Si_2C_2$ (and $Dy_3Si_2C_2$) the two Si–Si distances are practically the same with 248.7(3) and 249.4(3) pm (248.1(3) and 248.4(3) pm). In the hypothetical high-temperature structures, represented by the subcells, the Si–Si distances are equal; in $Pr_3Si_2C_2$ they are 251.9 pm. Thus, the differentiation of the two Si–Si distances in $Y_3Si_2C_2$, resulting in a shorter and in a longer Si–Si bond, is similar to the stabilization of low-temperature structures by Jahn-Teller or Peierls distortions.

The unweighted average of all Si–Si distances of the four refined structures is 249.8 pm. This distance is somewhat longer than the two-electron bond distance of 235.1 pm in the diamond structure of elemental silicon (17). It is also longer than the average two-electron bond distance Si–Si of 239 pm in the Zintl compounds Ca_5Si_3 (18) and the two modifications of $Ca_{0.65}Sr_{0.35}Si_2$ (19), i.e., $(Ca^{+2})_5(Si\text{–}Si)^{-6}$ Si^{-4} and $[(Ca_{0.65}Sr_{0.35})^{+2}]_2(Si_4)^{-4}$, which contain Si_2 pairs, Si_4 tetrahedra, and an infinite three-dimensional network of Si atoms, respectively. Thus, for simplicity we assign a bond order of one half to the Si–Si bonds, and since we can assume that the 3*s* and 3*p* orbitals fully participate in the bonding (octet rule), we obtain an oxidation number of -3 for the silicon atoms. Hence, in using the just assigned oxidation numbers (where shared bonding electrons are always *counted* at the atoms with the higher electronegativity) for the carbon and the silicon atoms, in a first approximation we obtain the simple formula $(R^{+3})_3(Si^{-3})_2(C_2^{-3})$.

In fine-tuning this unrefined model we have to consider that there is some weak *R*–*R* bonding, as discussed above. This can be accomplished only if the *R* atoms retain some electrons for *R*–*R* bonding bands. In this context we refer to the discussion of bonding in the Pr_2ReC_2 type carbides, where similar weak *R*–*R* bonding interactions must be assumed (20–22). Since the *R* atoms are the most electropositive components of the $R_3Si_2C_2$ silicide carbides, the Fermi level likely cuts through the only partially filled *R*–*R* bonding bands, and this may explain the metallic conductivity of these compounds reported in our earlier publication (1).[1] In Fig. 6 we present a more quantitative picture of the bond strength–bond length relationships for the Si–Si and C–C bonds than already given above. For a (one electron) Si–Si

[1] We want to take this opportunity to report a calibration error for one of the thermoelements in our SQUID magnetometer. After correction of this error, the Néel temperatures of the compounds $R_3Si_2C_2$ (R = Tb, Dy, Ho), determined from the magnetic susceptibility data, agree perfectly with the Néel temperatures as deduced from the electrical conductivity data of that publication (1).

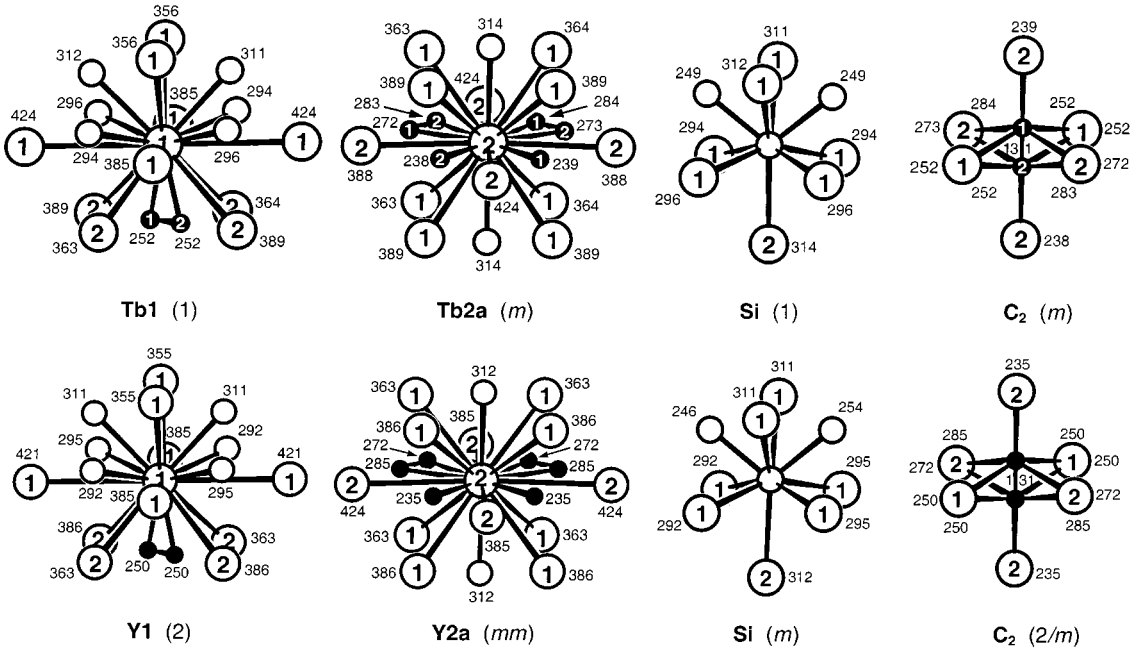

FIG. 5. Near-neighbor coordinations in the structures of $Tb_3Si_2C_2$ and $Y_3Si_2C_2$. The site symmetries of the central atoms are given in parentheses. Single-digit numbers correspond to the atom designations. Interatomic distances are given in pm units.

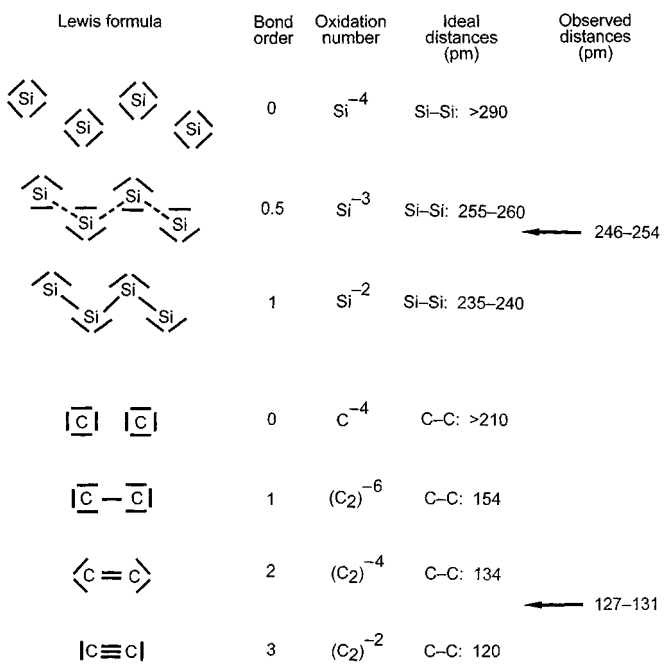

FIG. 6. Chemical bonding of the silicon zig-zag chains and the carbon pairs in the silicide carbides $R_3Si_3C_2$. The observed Si–Si distances correspond to bond orders somewhat higher than 0.5. For the C–C bonds of the carbon pairs bond orders of 2.5 or slightly less can be assigned. The electrons shown as lone pairs in the Lewis formulas are involved in *R*–Si and *R*–C bonding.

half-bond we have assumed a bond length of 255–260 pm from the experience with P–P bonds in polyphosphides (23–26), where a bond length of 221 $\pm$ 2 pm is found for P–P single bonds and about 245 pm for a (one-electron) P–P half-bond. Thus, for the same electron counts Si–Si bonds are about 20 pm longer than P–P bonds. If we correlate (by linear interpolation) the observed Si–Si bond lengths in the $R_3Si_2C_2$ compounds of between 246 and 254 pm (an average of 249.8 pm) with the "ideal distances" of 255–260 pm for a Si–Si half-bond and 235–240 pm for a single bond, we obtain an average Si–Si bond order of 0.65 and an average oxidation number of -2.7 for the silicon atoms. Similarly, for the carbon pairs in the compounds $R_3Si_2C_2$ with an average C–C distance of 129.6 pm a corresponding interpolation results in an average C–C bond order of 2.3 and an average oxidation number of -3.4 for the C_2 pairs. In using these oxidation numbers for the silicon atoms and carbon pairs we obtain (by charge compensation) an oxidation number of $+2.9$ for the average *R* atom, corresponding to the formula $(R^{+2.9})_3(Si^{-2.7})_2(C_2)^{-3.4}$. This account of chemical bonding may seem to be crude. It is based on the relative electronegativities of the elements, on the octet rule for silicon and carbon atoms, and on bond length–bond strength relationships. However, it allows us to understand the metallic conductivity of the $R_3Si_2C_2$ silicide carbides and no computer is needed for this rationalization.

ACKNOWLEDGMENTS

We thank the Deutsche Forschungsgemeinschaft, the Fonds der Chemischen Industrie, and the International Centre for Diffraction Data for the financial support of this work.

REFERENCES

1. M. H. Gerdes, A. M. Witte, W. Jeitschko, A. Lang, and B. Künnen, *J. Solid State Chem.* **138,** 201 (1998).
2. A. M. Witte and W. Jeitschko, *Z. Kristallogr. Suppl.* **10,** 96 (1995).
3. B. A. Frenz & Associates, Inc., and Enraf Nonius, SDP (Structure Determination Package), Version 3, College Station, Texas, and Delft, Holland, 1985.
4. G. M. Sheldrick, SHELXS-86, Computer Program for Crystal Structure Determination, Universität Göttingen, Germany, 1986.
5. G. M. Sheldrick, SHELXL-93, Computer Program for the Refinement of Crystal Structures, Universität Göttingen, Germany, 1993.
6. G. M. Sheldrick, SHELX-97, Program System for the Solution and Refinement of Crystal Structures, Universität Göttingen, Germany, 1997.
7. L. M. Gelato and E. Parthé, *J. Appl. Crystallogr.* **20,** 139 (1987).
8. R.-D. Hoffmann, *RWERT*—Program for the Calculation of Residuals for Different Classes of Reflections, University of Münster, Germany, 1996.
9. B. D. Cullity, "Elements of X-Ray Diffraction," Addison–Wesley, Reading, MA, 1959.
10. L. V. Azároff, "Elements of X-Ray Crystallography," McGraw–Hill, New York, 1968.
11. B. E. Warren, "X-Ray Diffraction," Addison–Wesley, Reading, MA, 1969.
12. M. Atoji, *J. Chem. Phys.* **54,** 3514 (1971).
13. H. Wondratschek and W. Jeitschko, *Acta Crystallogr. A* **32,** 664 (1976).
14. K. Yvon, W. Jeitschko, and E. Parthé, *J. Appl. Crystallogr.* **10,** 73 (1977).
15. K. Brandenburg, M. Berndt, and G. Bergerhoff, DIAMOND—Visuelles Informationssystem für Kristallstrukturen, Universität Bonn, Germany, 1999.
16. R. Pöttgen, D. Kaczorowski, and W. Jeitschko, *J. Mater. Chem.* **3,** 253 (1993).
17. J. Donohue, "The Structures of the Elements," Wiley, New York, 1974.
18. J. Evers, G. Oehlinger, and A. Weiss, *Z. Naturforsch.* **34b,** 358 (1979).
19. B. Eisenmann and H. Schäfer, *Z. Naturforsch.* **29b,** 460 (1974).
20. W. Jeitschko, G. Block, G. E. Kahnert, and R. K. Behrens, *J. Solid State Chem.* **89,** 191 (1990).
21. H. Deng and R. Hoffmann, *Inorg. Chem.* **32,** 1991 (1993).
22. M. H. Gerdes, W. Jeitschko, K. H. Wachtmann, and M. E. Danebrock, *J. Mater. Chem.* **7,** 2427 (1997).
23. H. G. V. Schnering and W. Hönle, *in* "Encyclopedia of Inorganic Chemistry," (R. B. King, Ed.), Wiley, London, 1994.
24. S. Rundqvist, private communication (1979).
25. M. V. Dewalsky, W. Jeitschko, and U. Wortmann, *Chem. Mater.* **3,** 315 (1991).
26. Th. Ebel and W. Jeitschko, *J. Solid State Chem.* **116,** 307 (1995).